An XPS study of iron sodium silicate glass surfaces

A. Mekki [a,b], D. Holland [a,*], C.F. McConville [a], M. Salim [b]

[a] Department of Physics, University of Warwick, Coventry CV4 7AL, UK
[b] Department of Physics, King Fahd University of Petroleum and Minerals, Dhahran 31261, Saudi Arabia

Abstract

A series of $(SiO_2)_{0.7-x}(Na_2O)_{0.3}(Fe_2O_3)_x$ glasses $(0.0 \leq x \leq 0.18)$ were prepared and investigated by means of X-ray photoelectron spectroscopy (XPS). The quantitative ratio $[Fe^{2+}]/[Fe_{total}]$, for each glass has been determined from an analysis of the Fe 3p spectra. For low Fe_2O_3 content both iron valencies are present, however, it was found that Fe^{3+} is the dominant species for high Fe_2O_3. From an analysis of the O 1s spectra, it was possible to discriminate between bridging and non-bridging oxygen atoms. It was found that the ratio of the non-bridging oxygen content to the total oxygen content increases with increasing iron concentration. It has also been shown that the non-bridging oxygen contribution to the O 1s spectra can be simulated by summing the contributions from the SiONa, SiOFe(II) and SiOFe(III) components present in the glass.

1. Introduction

The chemical analysis of glass surfaces by means of XPS has previously been applied to a study of the local structure of silicate, germanate, and phosphate-based glasses [1–4]. Iron sodium silicate glasses are mixed valence compounds in that they contain both oxidation states (Fe^{2+} and Fe^{3+}) and, as a result, have electrical and magnetic properties that are of particular technological importance [5–7]. In these glasses, the electronic conduction process is due to the hopping of a 3d electron from the Fe^{2+} to the Fe^{3+} ion. This unpaired electron induces a polarization of the lattice, and the charge carrier is in fact a polaron. For a description of the electrical conduc-

tivity in these types of materials, the Mott model is generally applied [5].

Recently, XPS has been applied to study the chemical effect of introducing iron into phosphate [2] and borate [8] glasses. In the case of phosphate glasses, high resolution XPS analysis has been performed in which both oxidation states of iron were systematically identified and the glass structure and other physical properties were also explained in terms of the valence states of iron and a quantitative analysis of the bridging to non-bridging oxygen concentration ratios. For the phosphate glasses, both Fe^{2+} and Fe^{3+} were observed to contribute to the non-bridging oxygen signal. For silicate glasses, however, Fe^{2+} exhibits a higher solubility and ionic diffusion than Fe^{3+}, suggesting that the Fe^{3+} may play an intermediate role in these glasses. If this is indeed the case, then oxygens in the unit SiOFe(III) should have a more covalent character, and the O 1s

* Corresponding author. Tel.: +44-1203 523 396; fax: +44-1203 692 016; e-mail: phsay@csv.warwick.ac.uk.

level might well be expected to show binding energies more typical of bridging rather than the non-bridging oxygens of SiOFe(II). In order to resolve this problem, this paper reports an investigation of the redox state of iron and the local structure surrounding the oxygen atoms in a series of sodium silicate-based glasses doped with various amounts of Fe_2O_3.

2. Experimental procedures

The compositions of the glasses produced can be expressed by the general formula, $(SiO_2)_{0.70-x}$-$(Na_2O)_{0.30}(Fe_2O_3)_x$, where $x = 0$, 0.05, 0.10, 0.15, and 0.20. Analytical grade powders of Fe_2O_3, Na_2CO_3 (for Na_2O) and SiO_2, in the required stoichiometric ratios, were melted in a platinum crucible at temperatures ranging from 1300–1400°C, depending on the composition. The melts were cast into preshaped graphite-coated steel moulds yielding glass rod specimens with dimensions of $6 \times 6 \times 30$ mm³. These glass bars were annealed to 50°C below their glass transition temperature (T_g determined from differential thermal analysis DTA) for 2 h and then cooled to room temperature at a rate of 30°C per hour. X-ray diffraction patterns were taken for the five compositions to check for the presence of crystalline phases, and none could be detected. The samples were then stored in a desiccator in order to minimise water absorption.

The chemical compositions of the glasses were determined by a combination of inductively coupled plasma (ICP) emission spectroscopy and Rutherford backscattering spectroscopy (RBS). The results from both of these techniques were consistent and are used throughout this paper. Each composition was analysed at least twice and the estimated relative uncertainty in both techniques is about $\pm 5\%$ of the value. Table 1 lists the batch and analysed glass compositions obtained from the ICP results. Several properties of each glass were measured. Glass transition temperatures (T_g) were determined using DTA, and thermal expansion coefficients (α) were determined in the temperature range of 50–300°C using dilatometry. The expansion coefficient was also measured relative to that of silica and the necessary correction applied [9].

Table 1
Compositions of the nominally prepared and analyzed sodium iron silicate glasses. The relative uncertainty in the ICP results is $\pm 5\%$

x	Nominal			Analysed		
	Na_2O	SiO_2	Fe_2O_3	Na_2O	SiO_2	Fe_2O_3
0.00	0.30	0.70	–	0.306	0.694	–
0.05	0.30	0.65	0.05	0.287	0.667	0.046
0.1	0.30	0.60	0.10	0.298	0.618	0.085
0.15	0.30	0.55	0.15	0.304	0.563	0.13
0.2	0.30	0.50	0.20	0.299	0.517	0.18

XPS spectra from the C 1s, Fe 2p, Fe 3p, Si 2p, O 1s and Na 1s core-levels were recorded using a VG Scientific ESCALAB Mk II system, with appropriate computer controlled data collection, that has been described elsewhere [10]. The base pressure in both the preparation and spectrometer vessels was less than 5×10^{-10} mbar. XPS spectra were obtained using un-monochromated Al Kα radiation, operated at 130 W, and a 100 mm concentric hemispherical analyser. A period of approximately 3 h was required to collect the necessary data set from each sample and during this time there was no evidence of any change in the oxidation state of the iron. The analyser was operated in a constant resolution mode with a pass energy of 10 eV and a reduced exit slit for high resolution spectroscopy (the analyser energy resolution was determined to be 0.9 eV), while a pass energy of 50 eV was used for routine survey scans. The energy scale of the spectrometer was calibrated using photoelectron lines: Cu $2p_{3/2} = 932.67$ eV and Au $4f_{7/2} = 83.98$ eV. Binding energies are referenced to the carbon 1s peak at a binding energy of 284.6 eV. This is a somewhat fortuitous peak which arises from hydrocarbon contaminants in the vacuum, and is generally accepted to be independent of the chemical state of the sample under investigation. Each sample was fractured in turn under ultra high vacuum (UHV) conditions prior to XPS analysis. This fracturing was performed for two reasons; firstly to minimise the possibility of atmospheric contamination (mainly oxygen and carbon contamination) of the surface, and secondly the fractured surface is considered to be the optimum means of producing a surface that is compositionally and stoichiometrically most representative of the bulk state of the glass.

All of the spectra presented in this paper have been corrected for the charging effect and the presence of any inelastic background. Where necessary the spectra have also been smoothed, deconvoluted and fitted using a non-linear least squares approach [11]. The deconvolution procedure was used to remove spectral broadening effects due to the natural line width of the X-ray source and to allow for Gaussian broadening introduced by the electron energy analyser. Information concerning the oxygen bonding was obtained by deconvoluting and fitting the O 1s spectrum to the weighted sum of two Gaussian–Lorentzian (G–L ratio = 30%) peaks representing bridging and non-bridging oxygen atoms. The Lorentzian component of the fitted spectrum arises from the natural peak shape while the Gaussian component represents the instrumental broadening contribution to the spectrum. Although this approach was successfully applied to the oxygen data, it proved not to be possible to analyse the stronger Fe 2p transitions in the same way due to the high inelastic background scattering present. However, a weak feature associated with the Fe 3p level at approximately 55 eV, with a low inelastic background, was used to monitor the valence state of the iron in the glasses. The proportion of iron in the two possible oxidation states was determined for each composition by this time resolving the Fe 3p spectrum into a weighted sum of two Gaussian–Lorentzian (G–L ratio = 30%) peaks arising from Fe^{2+} and Fe^{3+}. Several samples were analysed in order to confirm the reproducibility of these quantitative spectral deconvolutions for both the Fe 3p and O 1s spectra. The overall accuracy in the determination of the peak positions and chemical shifts was found to be < 0.2 eV.

3. Results

Survey scan X-ray photoelectron spectra for several glass compositions, obtained from the newly fractured surfaces, are shown in Fig. 1. The XPS and Auger peaks from the constituent elements in the glass are easily identified and are marked on the spectra. The presence of a very weak C 1s peak, due to contamination in the vacuum chamber, is also noted. A high resolution C 1s spectrum for a glass

sample with $x = 0.085$ is shown in Fig. 2. The spectra for the other glass compositions were similar to that of $x = 0.085$. As can be seen from Fig. 2, there is a single narrow, symmetric peak at a binding energy of 284.6 eV associated with background carbon contamination. Note that the C 1s signal associated with Na_2CO_3 has a higher binding energy of 289.3 eV [12]. The absence of this transition in the spectrum of Fig. 2 indicates that there is no bonded carbon in our glass sample and that all of the Na_2CO_3 has decomposed into CO_2, which has evaporated from the melt, leaving only Na_2O.

3.1. Iron spectra

It is well known for iron oxide surfaces that the core level spectrum of Fe^{2+} has a $2p_{3/2}$ binding energy of ~ 709.7 eV with a broad shake-up satel-

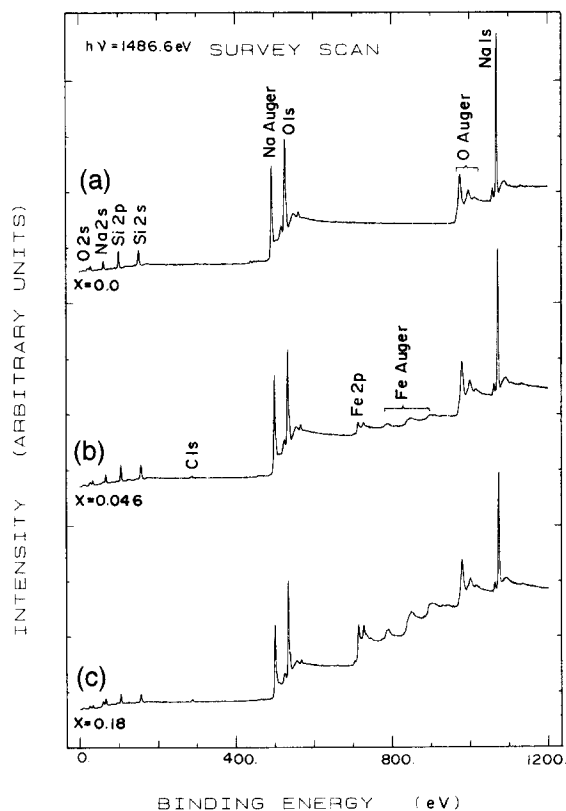Fig. 1. Survey scan XPS spectra ($h\nu = 1486.6$ eV) of three cleaved iron sodium silicate glasses with x values for the Fe_2O_3 content of (a) 0.0, (b) 0.046 and (c) 0.18.
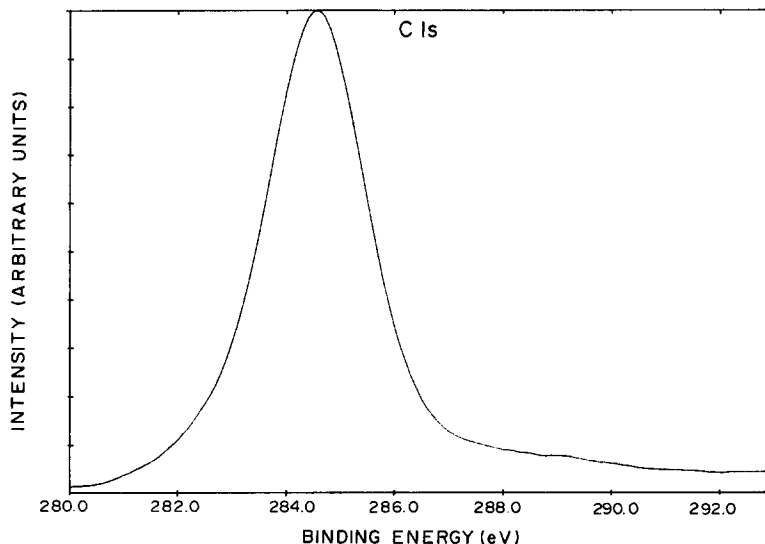
Fig. 2. High resolution C 1s spectrum recorded from a fractured glass sample containing 8.5% of Fe_2O_3 in the glass composition.

lite associated with it at a binding energy of ~ 715 eV [13]. In contrast, the core level spectrum of Fe^{3+} has a $2p_{3/2}$ binding energy of ~ 711.2 eV and associated broad shake-up satellite of binding energy ~ 719 eV [14]. Fig. 3 shows the high resolution Fe 2p spin–orbit doublet spectra for the analysed glass compositions. For glass compositions in which $x =$ 0.046 and 0.085, the Fe $2p_{3/2}$ peak is broad with a maximum at ~ 711 eV corresponding to the contribution from Fe^{3+} ions and a shoulder at ~ 709 eV due to electrons from the Fe^{2+} ions in the glass. As the iron content in the glass increases, this shoulder disappears and the peak narrows with the appearance of a broad satellite at ~ 719 eV characteristic of the Fe^{3+} species [13,14]. It was not possible to resolve the Fe 2p spectra due to the broad nature of the lines and the high background of the inelastically scattered electrons. However, it was possible to qualitatively deduce that in the case of low iron concentration, Fe^{2+} and Fe^{3+} species exist simultaneously in the glass, whereas for high iron concentration mostly Fe^{3+} species are present.

In order to quantify the valence state of iron in the silicate glasses, it was necessary to record and analyse the Fe 3p transition in relation to the iron content in the glass network. Each Fe 3p spectrum was resolved into two separate components. The formal charge difference between Fe^{2+} and Fe^{3+} is re-
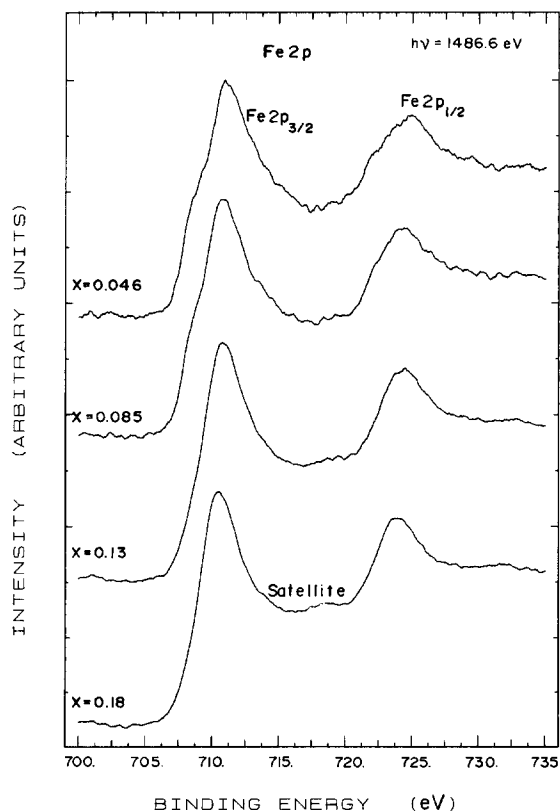

Fig. 3. A series of high resolution core level spectra from the Fe 2p transition for 4 glass compositions with x values for the Fe_2O_3 content ranging from 0.046 to 0.18.

flected in an energy shift of the Fe^{2+} transition to lower binding energies. The Fe 3p spectra for each glass composition are shown in Fig. 4(a) and two
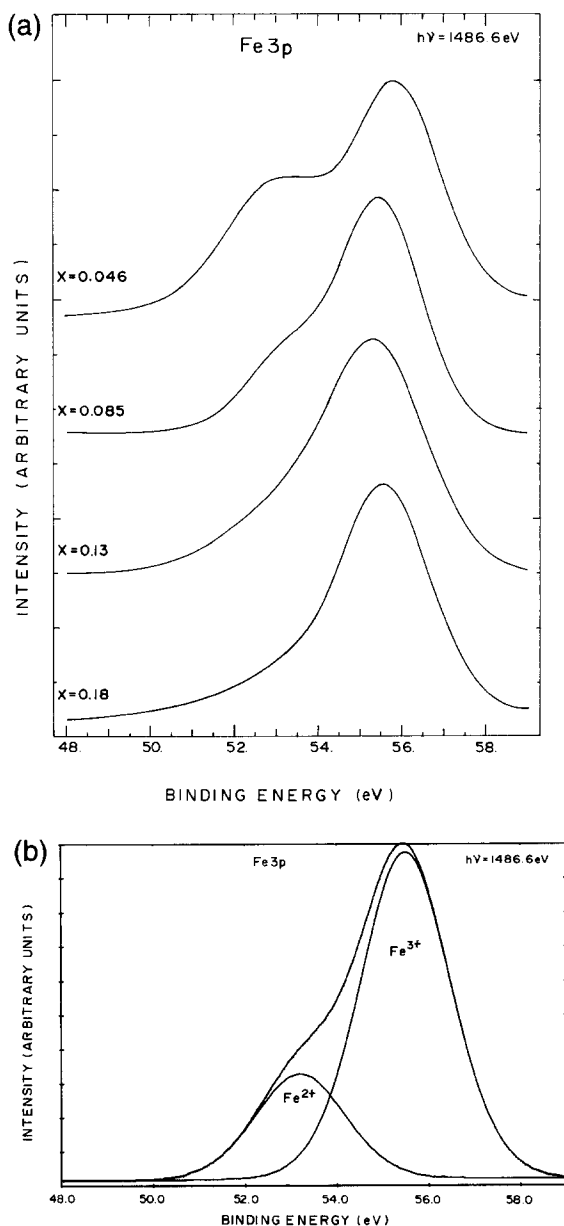

Table 2
Peak position for the core levels Fe 3p, Si 2p, and Na 1s for the iron sodium silicate glasses in eV; in parentheses are the FWHM of Si 2p and Na 1s peaks. The uncertainty in the measured ratio $[Fe^{2+}]/[Fe_{total}] = \pm 5\%$

| x | Fe 3p | | Si 2p | Na 1s | $[Fe^{2+}]/[Fe_{total}]$ |
	Fe^{2+}	Fe^{3+}			
0.0			102 (1.95)	1071.5 (2)	
0.046	53.75	55.9	101.6 (2)	1070.95 (2)	0.43
0.085	53	55.5	101.4 (2)	1070.95 (1.95)	0.23
0.13	53	55.35	101.3 (2.1)	1071.1 (2.1)	0.19
0.18	53	55.6	101.1 (2)	1070.1 (2)	0.09

distinct peaks are observed. The intensity of the lower binding energy transition decreases with increasing iron content and is attributed to Fe^{2+} ions. The second transition corresponds to Fe^{3+} ions in the glass. Fig. 4(b) shows the fitting of the Fe 3p high resolution spectrum for $x = 0.085$ to the sum of two weighted Gaussian–Lorentzian peaks (G–L ratio $= 30\%$) corresponding to contributions from the Fe^{2+} and Fe^{3+} species. Using these peak areas, the relative proportion of transition metal ions in each oxidation state can be determined. Table 2 summarises the data for the Fe 3p spectra relative to the Fe_2O_3 in the glass. As can be seen, the proportion of Fe^{2+} ions in the glass decreases with increasing Fe_2O_3 content.

3.2. Oxygen 1s spectra

In the case of the sodium silicate glass, it is well known that the Na_2O breaks up the SiO_4 tetrahedral network. Because of the extra oxygen atoms introduced with the Na_2O, not all the oxygens are joined to two Si atoms as they are in silica, some are bonded to only one silicon atom. These atoms are termed 'non-bridging' oxygens, while those linking two silicons are termed 'bridging' oxygens. The sodium ions are associated with the negatively charged non-bridging oxygen atoms $(Si-O^-Na^+)$. XPS has proved to be a powerful analytical technique that can be used to resolve the contributions to the O 1s core level spectrum from the bridging and non-bridging oxygen atoms in simple binary glasses, as well as in more complex glass systems [2–4]. The

Fig. 4. (a) High resolution core-level spectra from the Fe 3p transition for 4 glass compositions with x values for the Fe_2O_3 content ranging from 0.046 to 0.18. (b) The fitted Fe 3p spectrum for the $x = 0.085$ glass composition. The points are experimental data while the fitted components and their sums are represented by the continuous lines.

chemical shift associated with the photoelectron transitions is intimately linked with the effective atomic charge on the atoms probed. An *increase* in the electron density on the relevant atom screens the core electrons and hence *decreases* the measured
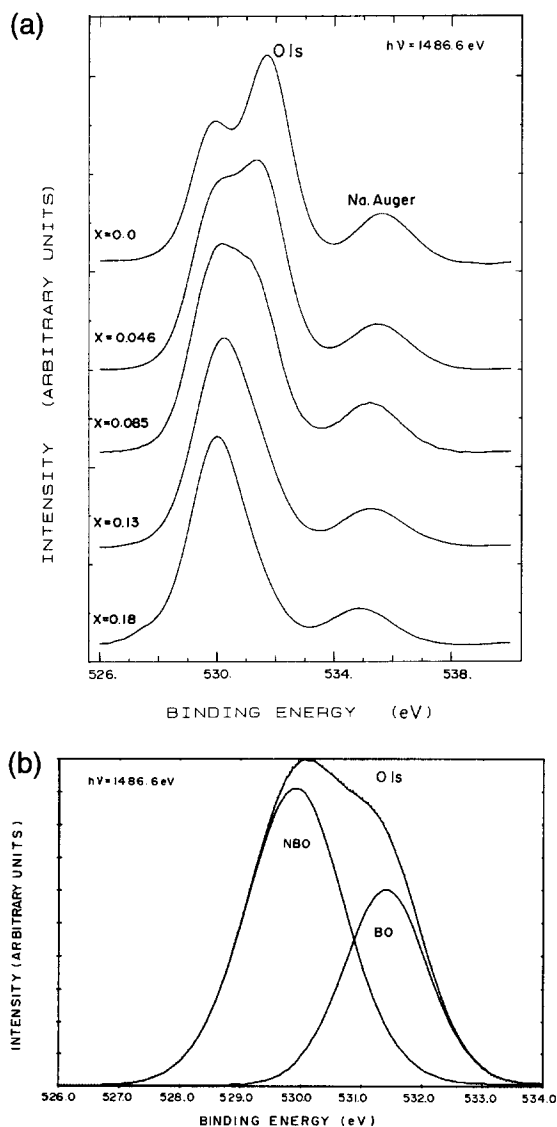

Fig. 6. Variation of the fitting parameters for the O 1s spectra as a function of Fe_2O_3 content in the glass.

Fig. 5. (a) High resolution core-level spectra of the O 1s for glass compositions with x values for the Fe_2O_3 content ranging from 0.0 to 0.18. (b) O 1s spectrum for the $x = 0.085$ glass composition. The points are the experimental data while the fitted components and their sums are represented by the continuous lines.
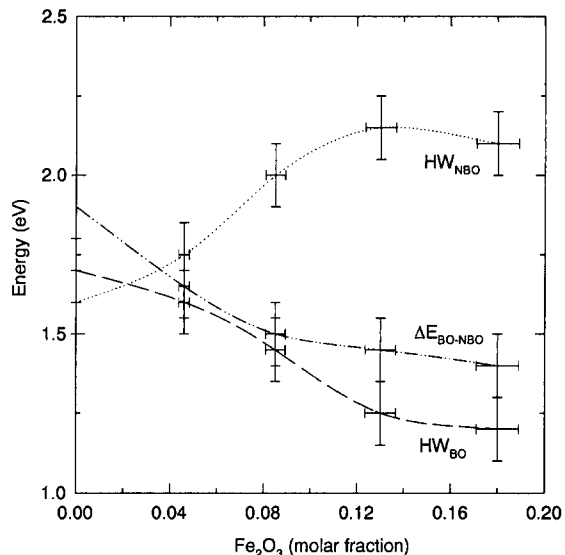
binding energy. Therefore, the low binding energy contribution to the O 1s spectrum is assigned to the non-bridging oxygen due to the effective charge on the oxygen atom in that environment being higher than that for the bridging oxygen atom.

The O 1s core level high resolution spectra for $0.0 \leq x \leq 0.18$ are shown in Fig. 5(a). There is significant compositional dependence within the spectra, and three distinct peaks are observed. The intensity of the high binding energy peak at ~ 536 eV, corresponds to the sodium $KL_1L_{2,3}$ Auger transition. The low binding energy peak at ~ 530 eV corresponds to the contribution from the non-bridging oxygen atoms, while the peak at ~ 532 eV is attributed to the bridging oxygen. As can be seen from Fig. 5(a), the addition of Fe_2O_3 to the $(Na_2O)_{0.30}(SiO_2)_{0.70}$ base glass system seems to result in an increase in the fraction of non-bridging oxygen atoms at the expense of the bridging oxygens. Previous studies (e.g., [1]) have established that the experimental ratio of non-bridging oxygen to the total oxygen for a glass composition of $(Na_2O)_{0.30}(SiO_2)_{0.70}$ is 38%. This is in excellent agreement with our findings where the calculated value from the glass composition is 36%. The O 1s spectrum, shown in Fig. 5(b) for $x = 0.085$, is simi-

lar to that of Yamanaka et al. [15] who investigated the Na_2O–TiO_2–SiO_2 system with TiO_2 substituted for SiO_2 These authors considered the O 1s spectrum to be composed of two overlapping peaks associated with bridging and non-bridging oxygen atoms. In the present work, each peak of the spectrum has been fitted to a sum of Gaussian–Lorentzian peaks (G–L ratio = 30%) similar to that shown in Fig. 5(b). A best fit of the data for each composition was found by varying the position, width and intensity of each of the two peaks. The results of the fitting parameters of the O 1s spectra are shown in Fig. 6.

The Si 2p spectra are shown in Fig. 7. It is clear from the figure that the peaks shift to lower binding energies as more iron is substituted for silicon into the glass. This shift is approximately 1.1 eV over the composition range studied. The Na 1s photoelectron
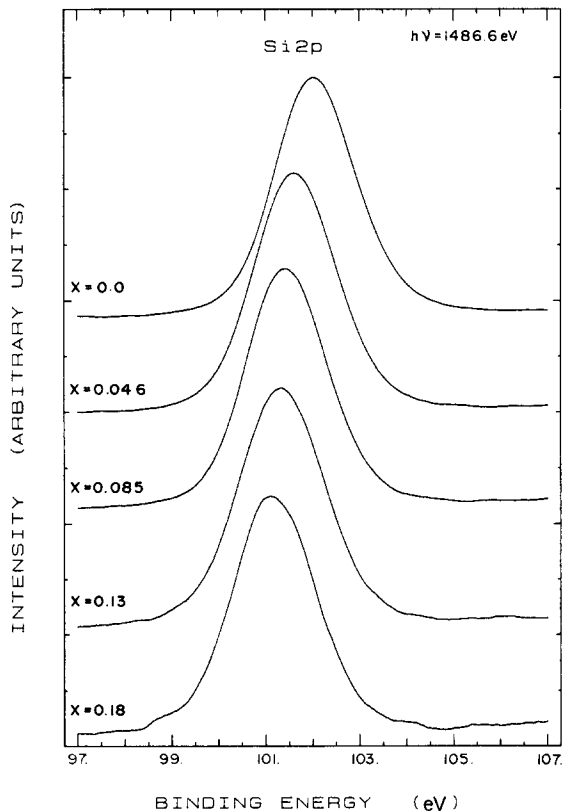

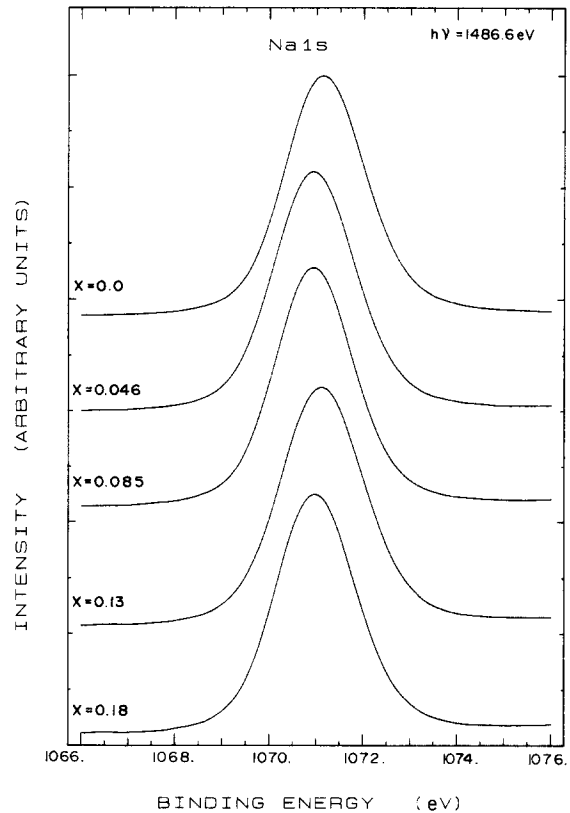
Fig. 8. Core level spectra from the Na 1s transition for glass compositions with x values for the Fe_2O_3 content ranging from 0.0 to 0.18.

Fig. 7. Core level spectra from the Si 2p transition for glass compositions with x values for the Fe_2O_3 content ranging from 0.0 to 0.18.

spectra for the glass compositions $0.0 \le x \le 0.18$ are also shown in Fig. 8. As seen from this figure, the Na peaks are symmetric with a full width at half maximum of ~ 2 eV for all compositions studied. Although there is a very small shift to lower binding energy with increasing iron content, this indicates that the sodium atoms exist in one bonding configuration. Fig. 9(a) and (b) show the dependence of the glass transition temperature (T_g) and thermal expansion coefficient (α) on the Fe_2O_3 content of the glass. It can be seen that T_g increases significantly up to $(Fe_2O_3)_{0.08}$, and then more slowly to $(Fe_2O_3)_{0.13}$ where it reaches a maximum and then begins to decrease. By contrast, the behaviour of α is almost opposite, decreasing slowly to a value of $(Fe_2O_3)_{0.05}$ and then more rapidly reaching a mini-
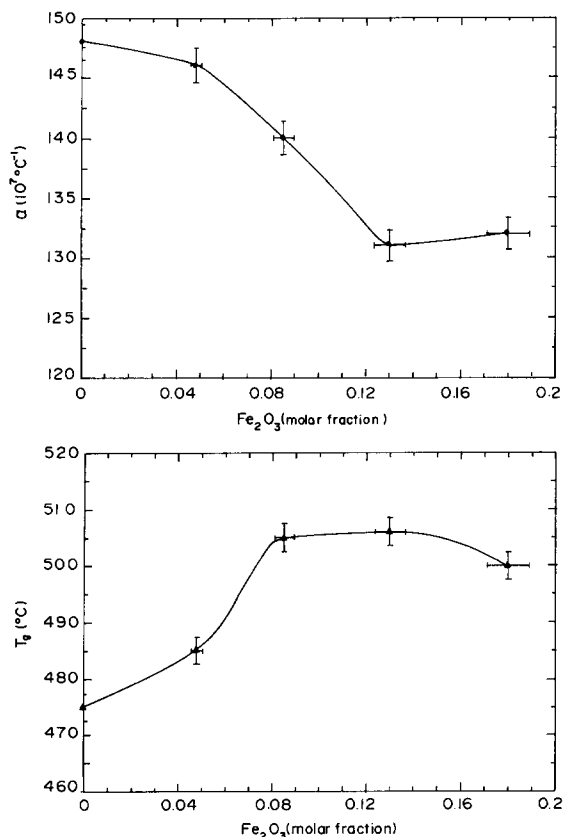
Fig. 9. (a) Glass transition temperature, and (b) thermal expansion coefficient versus Fe_2O_3 content in the glass. The solid line is drawn to guide the eye.

mum value at the same iron content in the glass ($x = 0.13$) after which it remains constant.

4. Discussion

The data obtained from the fitting of the O 1s spectra have been compared with the work of Goldman [16] who studied the effect of increasing the proportion of Fe^{2+} from 6% to 90%, on the non-bridging oxygen atoms in a $(Na_2O)_{0.18}(Si)_2)_{0.72}$-$(Fe_2O_3)_{0.10}$ glass composition. Goldman found that there was no change in the measured proportions of non-bridging oxygen atoms as an increased amount of Fe^{2+} was incorporated in the glass. As a result, the binding energy of the O 1s in the proximity of an iron atom was found to be independent of its oxida-

tion state. Similarly, the signal from the oxygen atoms in the SiOFe(III), SiOFe(II) and SiO^-Na^+ all contribute to the non-bridging oxygen signal and hence it was not possible to resolve contributions from the above three configurations.

The changes in fitting parameters of the O 1s transitions, as Fe_2O_3 is substituted for SiO_2 in the sodium silicate base glass, are summarised in Fig. 6. There is a decrease in the binding energy difference between bridging oxygen and non-bridging oxygen atoms indicating that the difference in chemical environment between the two sites becomes smaller. The half width of the bridging oxygen peak decreases linearly, while that of the non-bridging oxygen peak increases until $x = 0.13$, where it reaches a maximum value before decreasing. These changes reflect the decrease in the bridging oxygen signal and the increase in the non-bridging oxygen signal due to the contribution from SiOFe, when SiO_2 is substituted by Fe_2O_3 in the glass. This is in agreement with the previously published work by Goldman [16].

Table 3 shows the measured proportions of non-bridging oxygens determined using a two-peak fit for the O 1s spectrum. The non-bridging oxygen signal increases with increasing iron content in the glass. This increase suggests that the signal arising from SiOFe(III) systematically increases in the non-bridging region. This effect would suggest that Fe^{3+} is behaving as a network modifier and that the signal from oxygen atoms in SiOFe coincides with those in SiO^-Na^+ and that they are all contributing to the peak attributed to the non-bridging oxygen atoms. The energy difference between the above configurations is too small to be detected at the present resolution. The data in Table 3 shows the agreement between the calculated ratio (from Eq. (1)) and the

Table 3
Comparison between predicted and experimental compositional dependence of the fraction of non-bridging oxygen atoms in $(SiO_2)_{0.70-x}(Na_2O)_{0.30}(Fe_2O_3)_x$. The experimental values have an uncertainty of $\pm 5\%$

Comp. x	[NBO]/[O_T] measured	[NBO]/[O_T] predicted
0.0	0.38	0.35
0.046	0.46	0.48
0.085	0.64	0.61
0.13	0.8	0.74
0.18	0.88	0.89

experimental ratio for the non-bridging oxygen (NBO) and total oxygen (O_T) in the glass:

$$\frac{[NBO]}{[O_T]}$$

$$= \frac{2[Na_2O] + 6[Fe_2O_3] + 4[Fe_2O_2]}{[Na_2O] + 2[SiO_2] + 3[Fe_2O_3] + 2[Fe_2O_2]} \cdot \tag{1}$$

A similar shift to lower binding energy for the Si 2p level, as shown in Fig. 7, has also been observed by Veal et al. in the study of the Na_2O–CaO–SiO_2 system [17]. These authors attributed this downward shift to an increase in those atoms bonded to non-bridging oxygen atoms. The silicon atom at the centre of a tetrahedron of oxygen atoms is influenced by the bonding of those oxygens in the next coordination sphere. An electron contributed (ionically) from the sodium (or iron) to a non-bridging oxygen apparently enables this oxygen to relax its attractive potential toward the silicon atom, resulting in a greater electron density associated with these atoms. This relaxation effect has also been found to be important in preliminary theoretical cluster calculations [18].

There is a small change in the overall binding energy of the Na 1s core level peak with increasing iron substitution, as seen in Fig. 8. This effect sug-

gests that there is only a minor fluctuation in the charge distribution around the sodium atoms when iron is substituted for silicon in the base glass. The observed trends in the glass transition temperature and the thermal expansion coefficient are usually associated with the re-polymerization of the glass network, i.e., some intermediate behaviour of Fe^{3+}. However, this should imply the presence of more covalent SiOFe links (Fe and Si have the same Pauling electronegativities of about 1.8). Hence on the one hand, there is evidence of intermediate behaviour from the thermal expansion measurements whilst, on the other hand, there is also evidence of modifier behaviour from the XPS determination of the non-bridging oxygen content of the glasses. The data in Table 3 would tend to suggest that nearly all the oxygens are non-bridging at the highest iron content. This condition is not consistent with the ability to form a glass, and an alternative interpretation of the XPS data must be found which takes account of the fact that Fe–O bonding is not purely ionic.

Let us consider the ratio, Z/r, of the ions bonded to the oxygens as a crude measure of their ability to remove charge from the oxygen and, thus, increase the O 1s binding energy (Z being the nominal charge on the ion and r being the radius in nm). The Z/r values are Si^{4+} (100.0), Na^+ (9.8), Fe^{2+} (32.8),
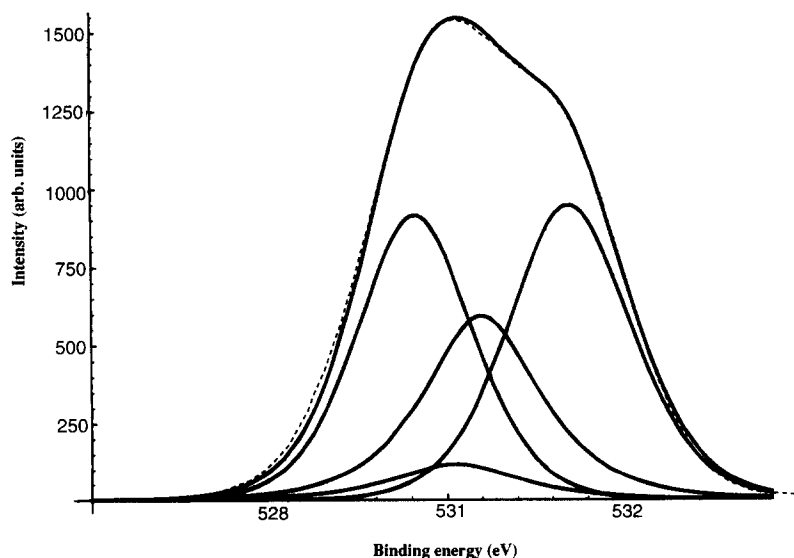

Fig. 10. Simulation of the O 1s spectrum with four peaks for 8.5% Fe_2O_3 glasses. The broken line represents the experimental data.

and Fe^{3+} (54.5), respectively. We can then use these numbers to derive values for the O 1s binding energies of the SiOFe(II) and SiOFe(III) contributions by a linear interpolation between the observed values for SiOSi and SiO^-Na^+ ($x = 0$). On this simple basis we would expect that, as iron oxide is substituted for SiO_2, the O 1s for the Si–O–Si configuration at 531.5 eV would be replaced by peaks for SiOFe(II) and SiOFe(III) at positions of approximately 530.2 eV and 530.5 eV, respectively. The SiO^-Na^+ peak can be considered to remain at 529.8 eV.

Fig. 10 shows the simulation of the O 1s peak based on the above model. This is produced using a Gaussian–Lorentzian function, with a ratio equal to the experimental value, a half-width based on the value from the $x = 0$ sample and intensities calculated from the chemical composition and the Fe^{2+}/Fe^{3+} ratios from the XPS data. The simulation shown is for the base glass doped with 8.5% Fe_2O_3. It is clear that this simple model, based on the chemistry and the composition of the glass accurately reproduces the experimental data for this glass composition, and the remaining glass compositions not shown here. We have therefore been able to go beyond the somewhat misleading concept of simple bridging and non-bridging oxygens by reproducing the experimental spectra using all the possible contributions to the O 1s XPS spectrum that are physically present in the glass.

5. Conclusion

XPS has been used to investigate the effect of substituting various amounts of Fe_2O_3 for SiO_2 in a $(Na_2O)_{0.30}(SiO_2)_{0.70}$ base glass. We have found that iron exists in both ferrous and ferric states in the sodium silicate glasses. The proportions of Fe(II) and Fe(III), in each glass sample, have been obtained by resolving the Fe 3p spectra and by measuring the relative ratio $[Fe^{2+}]/[Fe_{total}]$ which decreases when an increasing amount of Fe_2O_3 is substituted for SiO_2 in the base glass. From the O 1s XPS spectra it has been found that Fe(III) behaves as a glass modifier, which is somewhat in disagreement with the physical properties of the glass. This problem has been resolved by considering that the 'non-bridging

oxygens' contribution to the O 1s spectrum can be accurately simulated by summing the contributions from oxygens in SiO^-Na^+, SiOFe(II), and SiOFe(III). The choice of these components is based on structural considerations and all should be present in the glass. With the present level of instrumental resolution, it was not possible to discriminate these individual contributions because of the small binding energy differences between them.

Acknowledgements

References

[1] M.M.J. Smets and T.P.A. Lommen, J. Non-Cryst. Solids, 46 (1981) 21; Phys. Chem. Glasses 22 (1981) 158.

[2] R.K. Brow, C.M. Arens, X. Yu and E. Day, Phys. Chem. Glasses 35 (1994) 132.

[3] C.H. Hseih, H. Jain, A.C. Miller and E.I. Kamitsos, J. Non-Cryst. Solids 168 (1994) 247.

[4] R.K. Brow, R.J. Kirkpatrick and G.L. Turner, J. Am. Ceram. Soc. 73 (1990) 2293.

[5] N.F. Mott and E.A. Davis, Electronic Processes in Non-Crystalline Materials (Clarendon, Oxford, 1971).

[6] P. Gaskell and R. Ward, Trans. Metall. Soc., AIME 239 (1967) 269.

[7] K. Moorjani and J.M.D. Coey, Magnetic Glasses (Elsevier, Amsterdam, 1984).

[8] R. Kamal and S.W. Ali, J. Non-Cryst. Solids 87 (1986) 415.

[9] L.F. Olfield, Glass Technol. 5 (1964) 41.

[10] E.E. Khawaja, Z. Hussain, M.S. Jazzar and O.B. Dabbousi, J. Non-Cryst. Solids 93 (1987) 45.

[11] A. Proctor and P.M.A. Sherwood, Anal. Chem. 52 (1980) 2315.

[12] J.S. Hammond, J.W. Holubka, J.E. De Vries and R.A. Duckie, Corros. Sci. 21 (1981) 239.

[13] C.R. Brundle, T.J. Chuang and K. Wandelt, Surf. Sci. 68 (1977) 459.

[14] K. Wandelt, Surf. Sci. Rep. 2 (1982) 1.

[15] H. Yamanaka, K. Nakahata and R. Terai, J. Non-Cryst. Solids 95&96 (1987) 405.

[16] D.S. Goldman, Phys. Chem. Glasses 17 (1986) 128.

[17] B.W. Veal, D.J. Lam and A.P. Paulikas, J. Non-Cryst. Solids 49 (1982) 309.

[18] B.W. Veal and D.J. Lam, in: Proc. Int. Conf. on Physics of Si_2O and its Interfaces, ed. S. Pentelides (Pergamon, New York, 1978) p. 299.